Comparison of Rates and Kinetic Isotope Effects Using PEG-Modified Variants and Glycoforms of Glucose Oxidase: The Relationship of Modification of the Protein Envelope to C−H Activation and Tunneling†

Sean L. Seymour‡ and Judith P. Klinman*,‡,§

Department of Chemistry and Department of Molecular and Cell Biology, University of California, Berkeley, California 94720-1460

Received January 17, 2002; Revised Manuscript Received April 15, 2002

ABSTRACT: An earlier investigation of the temperature dependencies of rates and kinetic isotope effects (KIEs) in glucose oxidase (GO) used variants that differed in the extent of glycosylation at the surface of the protein. Kohen et al. [Kohen, A., Jonsson, T., and Klinman, J. P. (1997) *Biochemistry 36*, 2603−2611] presented evidence that the KIE on the Arrhenius prefactor varied as a function of protein modification, concluding that the degree of hydrogen tunneling at the active site was dependent on changes in mass at the surface. We now examine GO proteins containing polyethylene glycol (PEG) at their surface and a more extensively glycosylated form of GO, to distinguish simple mass effects from other sources of altered catalytic behavior. One PEG variant was created by modifying deglycosylated GO with short PEG chains (average of 350 Da each), while another contained a smaller number of long PEG chains (average of 5000 Da each). The light (146 kDa) and heavy (211 kDa) PEG variants and the hyperglycosylated variant display isotope effects on the Arrhenius prefactor that are similar (A_D/A_T = 0.55−0.62), while the unperturbed wild-type GO (WT-GO) is found to have an A_D/A_T that is reassessed as being close to unity. It appears that any modification of the protein surface away from that of the wild type gives rise to altered behavior for hydrogen transfer in the active site. We have also compared the effect of enthalpies of activation on both k_{cat}/K_M and k_{cat} for the variants, introducing a new method to extract the k_{cat}/K_M rate constant and enthalpy of activation for the tritiated substrate from competitive KIE experiments. We find similar trends in $\Delta H^{\ddagger}$ for both competitive and noncompetitive parameters and a smaller trend in k_{cat} than reported earlier. Correlations are observed between A_D/A_T and both the enthalpies of activation and the thermal melt temperatures (T_M) of the GO isoforms. In addition to the present study, there are now a number of examples where a perturbation of enzyme structure away from that of the wild type causes the observed KIE to become more temperature-dependent. The implications of these findings are discussed in the context of hydrogen tunneling and the relationship of protein structure and dynamics to this process.

In recent years, this laboratory has become engaged in an investigation of a possible role for protein conformational dynamics in enzymatic bond cleavage events (*1*−*3*). There are currently many methods available for studying the time evolution of motions within a protein, including multiple-photon echo spectroscopy (*4*−*6*), single-molecule techniques (*7*, *8*), neutron scattering methods (*9*, *10*), and time-resolved X-ray crystallography (*11*). The characterization of the dynamics of the chemical step in enzyme reactions can also be achieved, once it is possible to eliminate partial limitation by other steps during catalytic turnover. The most difficult challenge is to establish a definitive correlation between chemical dynamics and some critical element of protein or solvent conformational dynamics. A study of single molecules of cholesterol oxidase by Xie and co-workers (*12*) involved the simultaneous monitoring of reaction and conformational dynamics, showing that a motion slower than catalysis was altering the flavin reduction step. We are particularly interested in what role, if any, protein motions faster than the catalytic rate may play in modulating the energetic barrier in the chemical step. This type of participation of conformational dynamics can be distinguished by the terms "passive dynamics" and "active dynamics", with the former representing a sampling of multiple energy minima in the conformational landscape and the latter allowing the attainment of specific nonequilibrium configurations that facilitate catalysis (*13*−*25*). While it has been argued that the contribution of conformational dynamics to enzyme reactivity is unlikely to differ from effects in solution (*26*), this fails to take into account the very significant differences in structural elements within a protein versus bulk solvent.

Hydrogen transfer via quantum mechanical tunneling offers an excellent probe of conformational dynamics, due to the extreme sensitivity of tunneling to the shape of the

† This research was supported by a grant from the National Science Foundation (MCB 9816791) and the National Institutes of Health (GM 25765) to J.P.K.

* To whom correspondence should be addressed. Telephone: (510) 642-2668. Fax: (510) 643-6232. E-mail: klinman@socrates.berkeley.edu.

‡ Department of Chemistry.

§ Department of Molecular and Cell Biology.

10.1021/bi020054g CCC: $22.00
Published on Web 06/14/2002

reaction coordinate. The primary experimental tools for the detection of tunneling include the Swain-Schaad exponent (*27*), which describes the relationship among the rates for all three isotopes of hydrogen, and the measurement of the temperature dependence of kinetic isotope effects (KIEs)[1] (*2*, *28*). These can be determined at the same time using various isotopic combinations in a doubly radiolabeled competitive KIE experiment (*29*). Observed experimental parameters that deviate from the predicted limits of classical behavior have been previously documented in the literature (*2*). Although the theoretical basis for understanding the nature of hydrogen tunneling in enzymes is not fully resolved, it is clear that these characterizations can give a far more detailed description of the nature of the chemical step than was previously available.

As we describe in this paper, we have altered the surface of a protein and examined its effect on hydrogen transfer at a site far removed from the modification. The initial work of Kohen et al. (*1*, *30*) examined the influence of varied degrees of glycosylation at the protein surface on the oxidation of 2-deoxyglucose by glucose oxidase (GO). Wild-type glucose oxidase from *Aspergillus niger* (WT) is a homodimer with a molecular mass 155 kDa and catalyzes the oxidation of glucose to the δ-gluconolactone using a tightly bound FAD cofactor (*31*, *32*). Use of 2-deoxyglucose as a substrate allows kinetic access to a largely rate-limiting H-transfer step (*31*). In the study presented here, additional surface variants of recombinant GO have been prepared and characterized, in particular, those that contain the artificial polymer polyethylene glycol (PEG). As we now show, all surface modifications of GO beyond that of the wild-type enzyme give rise to altered behavior for hydrogen transfer in the active site such that the KIE becomes more temperature-dependent upon perturbation. This trend is discussed in the context of two other classes of enzyme reactions (*3*, *33*), where deviations from wild-type conditions have been found to lead to a similar increase in the temperature dependence of measured isotope effects.

EXPERIMENTAL PROCEDURES

Materials

[1-^{3}H]-2-Deoxyglucose (10 Ci/mmol) was purchased from Amersham Pharmacia Biotech. [U-^{14}C]-2-Deoxyglucose (340 mCi/mmol) was from American Radiolabeled Chemicals, Inc. Methoxy-PEG succinoyloxysuccinimide (mSSA-PEG) reagents, mSSA-PEG-350 and mSSA-PEG-5000, were purchased from Shearwater Polymer, Inc. Fluorescamine, cyclohexene, and bromine were from Aldrich. 2-Deoxyglucose (grade III) and bis-tris-propane were from Sigma. Sodium borodeuteride (99.83% D) was purchased from Cambridge Isotope Laboratories. Tetrabutylammonium dihydrogen phosphate concentrate (ion pair chromatography grade in sealed ampules) was from Fluka Chemika. The pH of all buffers was adjusted at the experimental temperature.

Endoglycosidase H (Endo H_f, 100 units/mL) was purchased from New England Biolabs. Hexokinase (3000 units/mL suspension), α-mannosidase (50 units/mL suspension), and glucose oxidase from *A. niger* (296 units/mg) were from Boehringer Mannheim. Recombinant glucose oxidase was prepared by A. Kohen using a yeast expression system (*34*) provided by S. Rosenberg, formerly of Chiron Corp. (Emeryville, CA). The exact plasmid, pαGO-1, used to produce the Rec GO with an approximate molecular mass of 205 kDa employed in the previous study was no longer available, and in its place we used plasmid pSGO2, also characterized in ref *34*. Expression with this plasmid yielded a protein with an average molecular mass of 320 kDa which was used as the parent protein in all preparations described in the current study. We note this distinction by referring to this protein as Rec320 GO and that in the previous study as Rec205 GO. Deglycosylated recombinant GO and [U-^{14}C,1-^{2}H]-2-deoxyglucose were prepared and characterized following the procedure described by Kohen et al. (*1*) and references therein, the exception being that the deglycosylated GO was from Rec320 (denoted Degly320 GO throughout).

Synthesis of [1-^{2}H]-2-Deoxyglucose. The cold deuterated substrate was prepared by the bromine−water oxidation of 2-deoxyglucose to the δ-lactone (*35*), followed by sodium borodeuteride reduction back to the sugar (*36*), accomplishing the net exchange of H for D in the anomeric position. This method was substituted for the published procedure (*1*) as it avoids the generation of mercury. The details of this synthesis are included in the Supporting Information.

Preparation of Polyethylene Glycol-Modified Deglycosylated Glucose Oxidases. Surface-accessible primary amines (15 lysines and the one N-terminus per monomer, all on the surface at least 15 Å away from the active site) of Degly320 GO were reacted with two different PEG functionalizing reagents, differing only in the average length of the polymer chain. The reaction of mSSA-PEG-350 with Degly GO was conducted as follows. To 2 mL of 50 μM Degly GO (800 μM in primary amines) in 100 mM KP_i (pH 8.8) was added 40 μL of mSSA-PEG-350 (an at least 100-fold molar excess). The pH was checked immediately and was returned to 8.8 with several 1 μL additions of 6 M NaOH. The reaction was allowed to proceed for 20 min, and the mixture was then dialyzed overnight against 100 mM KP_i (pH 6.5) using a 10 kDa cutoff Slide-A-Lyzer (Pierce Chemical Co.). The reaction of mSSA-PEG-5000 with Degly GO followed the same procedure, except that 80 mg of the solid mSSA-PEG-5000 reagent (100-fold molar excess over primary amines) was used. The extent of modification of available sites on the surface of the protein was determined for both generated proteins using the fluorescamine assay (*37*−*39*). It should be noted that all modified GOs examined in this study or in previous studies from this laboratory are expected to reflect a mixture of forms, due to the nature of the derivitization processes. The properties reported reflect those of the ensemble in each case.

Methods

In general, the methods used for enzyme concentration determination, competitive KIE experiments, initial velocity

[1] Abbreviations: GO, glucose oxidase; H, protium (^{1}H); D, deuterium (^{2}H); T, tritium (^{3}H); L, either H or D; *R*, gas constant; KIE, kinetic isotope effect; PEG, polyethylene glycol; Rec320 GO, recombinant GO with a mass of 320 kDa; Rec205 GO, recombinant GO with a mass of 205 kDa; Degly320 GO, deglycosylated GO from the Rec320 GO parent protein; Degly205 GO, deglycosylated GO from the Rec205 GO parent protein; PEG-350 GO, Degly320 GO modified with PEG chains with an average size of 350 Da; PEG-5000 GO, Degly320 GO modified with PEG chains with an average size of 5000 Da.

measurements, and temperature dependence analyses were described in Kohen et al. (*1*) with the specific additions and modifications as listed below. All GO concentrations are given per active site (per monomer), although the functional protein is a dimer. Data fitting was performed using KaleidaGraph by Synergy Software. All errors are one standard deviation.

Competitive Kinetic Isotope Effect Experiments. This study involved a careful examination of the influence of protium contamination in the deuterium substrates, using the methods described in refs *40* and *41*. Several refinements to this method and the competitive KIE experiment were made and are discussed in detail (*42*). As shown in the Supporting Information, a very large number of KIE measurements were determined for each enzyme form as a function of temperature varying from 24 measurements (wild type) to 121 (Degly320).

Temperature Dependence of Competitive Kinetic Isotope Effects. Instead of ecological regression being performed, i.e., regression on the average KIE at each temperature with weighting from the standard deviation of each, all the determinations at each temperature were plotted directly (*43*). The data were fitted two different ways. First, the data were analyzed by nonlinear regression to the Arrhenius KIE equation as previously done:

$$\mathrm{KIE}\left(\frac{\mathrm{L}}{\mathrm{T}}\right) = \left(\frac{A_\mathrm{L}}{A_\mathrm{T}}\right)\mathrm{e}^{\Delta\Delta H^{\ddagger}_{(\mathrm{T-L})}/RT} \qquad (1)$$

where the KIE is a function of temperature, $\Delta\Delta H^{\ddagger}_{(\mathrm{T-L})}$ the difference in the enthalpy of activation between the heavy isotope (T) and the light isotope (H or D), and $A_\mathrm{L}/A_\mathrm{T}$ the apparent isotope effect on the Arrhenius prefactor. Second, the Lowess method (*72*), which finds a moving average through the data rather than a fit to an assumed mathematical model, was also used to assess deviation from a simple exponential relation.

Determination of the Enthalpy of Activation on k_{cat} for [1-^{2}H]-2-Deoxyglucose. The anomerically deuterated analogue of 2-deoxyglucose was synthesized as described above. Using a YSI model 5300 oxygen uptake monitor, the steady state initial velocity was determined for eight temperatures from 4 to 45 °C under oxygen saturation with [1-^{2}H]-2-deoxyglucose at approximately 10-fold over its apparent K_M. Using $k_\mathrm{cat}/K_\mathrm{M}$ data for both oxygen and 2-deoxyglucose from this work and the previous study from this lab (*1*), the measurements were corrected to give the true k_cat (both substrates at infinite concentration) using the appropriate equation for a ping-pong mechanism (*44*):

$$k_\mathrm{cat} = \left[\frac{1}{(v/[\mathrm{enz}])_\mathrm{obs}} - \frac{1}{(k_\mathrm{cat}/K_\mathrm{M})_\mathrm{sugar}[\mathrm{sugar}]} - \frac{1}{[k_\mathrm{cat}/K_\mathrm{M})_{\mathrm{O}_2}[\mathrm{O}_2]}\right]^{-1} \qquad (2)$$

Measurement of the Thermal Melting Temperature. The thermal melting temperature (T_M) was determined for each of the five proteins in this study using an Aviv 62DS instrument to monitor the change in circular dichroism (CD) signal at 220 nm, heating from 3 to 81 °C in 1.5 °C steps at 1 °C/min followed by equilibration for 1.5 min at each step, and signal averaging for 40 s. The T_M was determined as described in ref *45* for two different pHs.

Determination of the Enthalpy of Activation on k_{cat}/K_M from Competitive Isotope Effect Data. The fractional conversion for the reaction of both isotopes versus time was determined for all competitive KIE experiments. For lower temperatures, the data fit a single-exponential increase with a rate constant, k_rate, equal to $k_\mathrm{cat}/K_\mathrm{M}$ times the enzyme concentration, E_0. At higher temperatures, some slow kinetic inactivation of the enzyme was indicated by non-single-exponential behavior and the incompleteness of the reaction at infinite time. If we assume the decrease in enzyme concentration is a first-order process with the rate constant k_inact, the k_rate can still be determined by fitting fractional conversion, f, versus time, t, using eq 3:

$$f = 1 - e^{-\frac{k_{rate}}{k_{inact}}\left(1-e^{-k_{inact}*t}\right)} \qquad (3)$$

The derivation of this equation is provided in the Appendix. In this manner, the value of $k_\mathrm{cat}/K_\mathrm{M}$ could be determined for H, D, and T substrates as a function of temperature, and $\Delta H^{\ddagger}$ could be determined from the fit of nonlinear regression to the Arrhenius equation:

$$\mathrm{rate} = (A)\mathrm{e}^{-E_\mathrm{a}/RT} \qquad (4)$$

where E_a is the activation energy and $\Delta H^{\ddagger} = E_\mathrm{a} - RT$. The errors in $k_\mathrm{cat}/K_\mathrm{M}$ at each temperature were taken from the fit to eq 3. The determination of the T_M for each protein indicated a significant fraction of the unfolded state at the highest temperatures in the experimental range. For this reason, all temperatures with any significant loss of initial enzyme concentration due to thermal denaturation were excluded from the fit.

RESULTS

Generation and Characterization of Surface Variants of Glucose Oxidase. The primary intent at the beginning of this study was to create a parallel series to the initial study of variably glycosylated GOs (*1*), by the addition of an artificial polymer (polyethylene glycol) to the surface of GO. Deglycosylated GO (Degly GO), obtained from the parent recombinant protein (Rec GO), was used to generate PEG-modified variants. The Rec GO used in earlier studies (*1*) was unavailable for the generation of Degly GO. Thus, Degly GO in this study is derived from a larger variant, Rec320 GO, and is denoted Degly320 GO. N-Terminal and DNA sequencing indicated that the Rec320 GO differed from the Rec205 GO solely in the extent of glycosylation on the surface. While Rec320 and Rec205 are clearly physically different, the Degly proteins derived from the parent proteins look similar on gels and are assumed to be almost identical. The origin or method of construction of each of the five proteins examined in the present study is listed in Table 1.

The characterization of the PEG-5000 GO and the PEG-350 GO with the fluorescamine assay (cf. Experimental Procedures) indicated modification of ca. 50 and 85% of available primary amine sites on the surface of GO (15 lysines and the N-terminus, leading to 32 primary amines per dimer), respectively. This translates into resultant average

Table 1: Description and Properties of Surface Variants of Glucose Oxidase

enzyme	origin or construction	MW (kDa[a,b])	no. of sites/MW of group[c]	D/T KIE[d] at 33 °C	k_{cat} (s^{-1})[e] at 33 °C
Rec320 GO	recombinant expression in yeast	320 ± 50[b]	10/19	2.23 ± 0.07	6.1 ± 0.3
Degly320 GO	deglycosylated Rec320 GO	136 ± 2[b]	10/0.30	2.26 ± 0.05	5.9 ± 0.3
PEG-350 GO	Degly320 GO with PEG-350 reagent	146 ± 4	27/0.35	2.22 ± 0.09	6.3 ± 0.3
PEG-5000 GO	Degly320 GO with PEG-5000 reagent	211 ± 20	15/5.0	2.25 ± 0.06	5.5 ± 0.3
WT GO	*A. niger*	155 ± 10[b]	10/1.9	2.24 ± 0.04	5.2 ± 0.3

[a] Reported per dimeric unit. The average MW as determined by SDS−PAGE for the glycoforms and using the fluorescamine assay for the PEG proteins. [b] The reported range approximates the MW distribution as seen on the gel. [c] The average number of occupied attachment points on the surface of the protein, reported per dimeric unit. The number of glycosylation sites is from the crystal structure of Degly GO. The number of occupied sites for PEG proteins as determined by the fluorescamine assay. The second number reports the average MW of the attached group in kilodaltons. [d] D/T KIE from competitive KIE experiments in 10 mM bis-tris-propane at pH 9.0. [e] Measured by the rate of O_2 uptake with [1-^{2}H]-2-deoxyglucose at pH 9.0 in 10 mM bis-tris-propane.

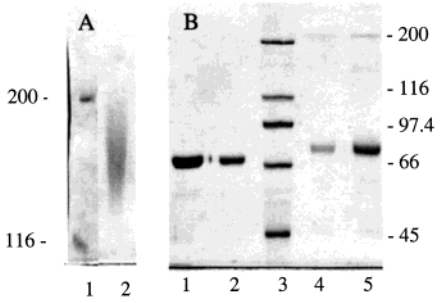

FIGURE 1: SDS−PAGE protein gels (6.87% acrylamide). (A) Lane 1, MW standards; and lane 2, PEG-5000 GO. (B) Lanes 1 and 2, Degly320 GO; lane 3, MW standards as indicated at the right of the gel; and lanes 4 and 5, PEG-350 GO.

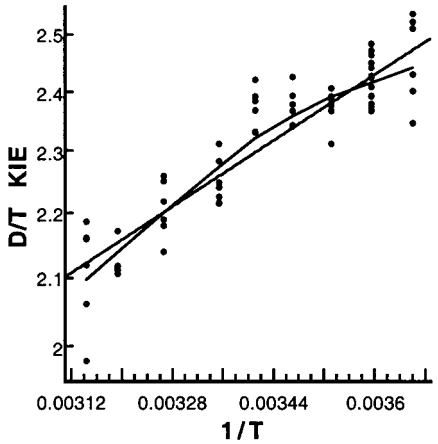

FIGURE 2: Example of detection of deviation from linear Arrhenius behavior. The D/T KIE for Rec320 GO is shown in logarithmic scale vs the inverse absolute temperature. The straight line is a fit to the Arrhenius isotope effect equation. The other fit is a Lowess regression, as described in Experimental Procedures.

molecular masses of 211 kDa for PEG-5000 GO and 146 kDa for PEG-350 GO. SDS−PAGE indicated that the larger PEG protein is a rather broad distribution of masses, as shown in Figure 1A, with an apparent average subunit molecular mass of ca. 160 kDa. This type of behavior, in which one observes a broad distribution of bands that run at an "aberrant" molecular mass, has been previously reported for proteins modified with PEG (*46*). The smaller PEG protein was found to be much more homogeneous, as shown in Figure 1B. The average molecular mass and estimated range, as well as estimates of the number and size of modifying groups on each of the five proteins studied in the present work, are given in Table 1. Also presented in this table are representative rates and KIEs for each of the GO variants (at 33 °C). Note that all the variants have KIEs that are within experimental error of one another, with differences among the enzymes only becoming statistically meaningful in the temperature dependencies of the KIEs when a substantial amount of data is examined. These differences are quite reproducible, as demonstrated and discussed in ref *42*. The temperature dependencies of all the D/T KIEs are available in the Supporting Information.

Curvature in the Temperature Dependence of Competitive KIEs. Full sets of data were collected for k_H/k_T and k_D/k_T as a function of temperature using each of the enzyme forms in Table 1. As discussed in earlier work, data for k_D/k_T can have significantly reduced kinetic complexity in relation to k_H/k_T (*47*, *48*). We noted that while the quantity of data obtained for some of the enzyme forms in this study was nearly double that acquired in the previous studies, analysis of data according to eq 1 did not decrease the error in A_D/A_T. This suggested that the choice of model to fit the data might be wrong. It became visibly clear that some of the log-scale plots of KIE were not completely linear versus $1/T$ and instead showed some downward curvature at low temperatures. The most obvious cause of curvature in these plots would be the onset of kinetic complexity at one end of the temperature range, attenuating the observed KIE at that end of the range below the intrinsic KIE and shifting the observed A_L/A_T away from the true value. To assess curvature in an unbiased fashion, the data were fitted by Lowess regression which finds a moving average through the data (*74*), rather than regression to a mathematical model. We used this fitting approach only to diagnose curvature, and no numerical results were derived from the Lowess fit. A comparison of a linear fit and a Lowess regression is shown in Figure 2 for Rec320 GO. In retrospect, careful inspection of the data shown in Figure 2 in an earlier publication (*1*) also reveals the suggestion of some downward curvature at low temperatures in both the H/T and D/T KIEs for some of the glycoforms. However, only with the greater amount of data reported here could curvature be resolved with certainty. This subsequent detection of curvature serves to emphasize that the statistical approach of doing many repetitions of a small number of *x* values is only appropriate when the model describing the data is known with certainty. This may not be the case in a temperature dependence study, due to the number of parameters that can change with temperature. The alternate approach of measuring many different temperature values is clearly preferable when the model may be equivocal (*49*).

Change in Kinetic Complexity with Temperature. With curvature in plots of KIE versus 1/*T* established for some of the enzyme forms, we attempted to distinguish which end of the temperature range was more altered by kinetic complexity and which was closer to the intrinsic behavior of the chemical step of the reaction. The following ping-pong mechanism can be written for GO where E_{ox} and E_{red}

Scheme 1

$$E_{ox} + S \underset{k_{-1}}{\overset{k_1}{\rightleftharpoons}} E_{ox}{\bullet}S \xrightarrow{k_2} E_{red}{\bullet}P \xrightarrow{k_3} E_{red} + P$$

$$E_{red} + O_2 \underset{k_{-4}}{\overset{k_4}{\rightleftharpoons}} E_{red}{\bullet}O_2 \xrightarrow{k_5} E_{ox} + H_2O_2$$

are the oxidized and reduced forms of the enzyme, S is the first substrate (2-deoxyglucose), and P is the first product (2-deoxygluconolactone). The macroscopic kinetic parameter k_{cat}/K_M for the first half-reaction will encompass all steps up to and including the first irreversible step (*50*). No reverse reaction of the chemical step, k_2, has ever been detected (*31*), so k_{cat}/K_M for the sugar can be written in terms of k_1, k_{-1}, and k_2 [$k_{cat}/K_{M(sugar)} = k_1k_2/(k_{-1} + k_2)$]. As competitive KIEs are always on k_{cat}/K_M (*50*), the attenuation of the observed competitive KIE below the intrinsic KIE on the chemical step (k_2) due to kinetic complexity is described by the following relationship (*51*):

$$\left(\frac{k_L}{k_T}\right)_{obs} = \frac{\frac{k_{2_L}}{k_{2_T}} + \frac{k_{2_L}}{k_{-1}}}{1 + \frac{k_{2_L}}{k_{-1}}} \qquad (5)$$

where $(k_L/k_T)_{obs}$ and (k_{2L}/k_{2T}) are the observed and intrinsic isotope effects, respectively.

The temperature dependence of the observed Swain-Schaad exponent can be used to ascertain the change in kinetic complexity with temperature, assuming the intrinsic value of the exponent is temperature-independent. In the classical limit, depression of the observed exponent below the predicted value for $(\ln k_H/k_T)/(\ln k_D/k_T)$ of 3.3 indicates kinetic complexity (*52*). In fact, the four enzyme forms that showed curvature in the temperature dependence of their D/T KIEs (Degly320 GO, Rec320 GO, PEG-350 GO, and PEG-5000 GO) also indicated a small decreasing trend with decreasing temperature in their observed exponents [e.g., from 3.31 at 45 °C to 3.20 at 0 °C, for Rec320 (data not shown)]. Thus, in the classical picture, these data suggest a small contribution of kinetic complexity at lower temperatures. We note that a change in kinetic complexity is not the only behavior that can modulate the Swain-Schaad exponent, and the observation of an exponent inflated above the classical value has been taken as evidence of the involvement of tunneling (*3*, *47*, *52*−*54*). However, in each of the experimental examples where sizable deviations from the classical Swain-Schaad exponent are observed (*3*, *52*−*54*), these appear in secondary isotope effects and not in the primary values such as those measured in this study.

This analysis of kinetic complexity was focused on the enzyme form with the greatest amount of data, Degly320. Comparison of single-turnover measurements of k_2 versus the observed k_{cat} at several temperatures with WT GO has indicated that the observed k_{cat} for [1-^{1}H]-2-deoxyglucose is virtually dominated by k_2 in Scheme 1, with the second half-reaction causing little limitation (*31*, *55*) of the expression for k_{cat}. Making the reasonable assumption that this is also true for the kinetically similar Degly320 GO, we compared the temperature dependence of noncompetitive deuterium isotope effects for Degly320 to the competitive H/T KIE. This analysis shows a reproducible break in the H/T KIEs with temperature, as well as a closer correspondence of the high-temperature H/T data to the k_{cat} data (*42*). Since the only rate constant that is common to k_{cat} and k_{cat}/K_M is k_2, this implies that k_2/k_{-1} is smaller at high temperatures, i.e., that the high-temperature region of the competitive KIE data approximates k_2.

The presence of a small commitment at lower temperatures implies that $\Delta H^{\ddagger}$ of k_{-1} is greater than that for k_2. As will be discussed later, the $\Delta H^{\ddagger}$ on k_2 is similar among all the enzyme forms, as inferred from the $\Delta H^{\ddagger}$ on k_{cat}. Thus, differences in the extent of change in commitment with temperature among the enzyme forms are expected to be controlled by differences in $\Delta H^{\ddagger}$ of k_{-1} such that an increasing level of alteration of the surface may increase the enthalpic barrier for substrate dissociation. In support of this notion, WT GO was found to have the least curvature in an Arrhenius plot of the D/T KIE, appearing close to perfectly linear (*1*). Additionally, the Swain-Schaad exponents for the WT are found to be nearly flat with temperature when examining data from Jonsson (*56*), Kohen et al. (*1*), and the present work. The PEG proteins, seen as the most drastically modified away from the WT, show the most apparent curvature in Arrhenius KIE plots of KIEs and small downward trends in the Swain-Schaad exponents at lower temperatures. Overall, the data imply that the WT has very little change in commitment with temperature, while the altered forms of GO show varying degrees of onset of kinetic complexity in k_{cat}/K_m at low temperatures.

Trend in A_D/A_T among the Enzyme Forms. The A_D/A_T parameters measured from the plots of D/T KIE versus 1/*T* are listed in Table 2 for each enzyme using the full temperature range (0−50 °C). On the basis of the above analysis of the change in commitment with temperature, we also report the A_D/A_T determined using only the higher two-thirds of the temperature range (15−50 °C) for the artificial variants of GO (second column of Table 2). The apparent trend in A_D/A_T is as follows: WT GO and Degly GO > Rec320 GO, PEG-5000 GO, and PEG-350 GO. The order of this trend is the same regardless of whether the full or limited temperature ranges are used. The trend is, however, more exaggerated in the latter case. In all further discussion and analyses, we use the estimates of the intrinsic A_D/A_T, listed in the second column of Table 2.

Table 2 also includes the results from two earlier studies of GO glycoforms analyzed in a similar fashion. The data from both are slightly different from those reported previously, as a result of being corrected for H contamination in D substrates. With the data of Kohen et al. (*1*), the trend in the A_D/A_T values is altered such that the Degly205 GO now lies below, as opposed to above, the WT GO. Although the A_D/A_T values in Jonsson (*56*) agree very well with the present study upon correction, the data from Kohen et al. (*1*) do not agree in absolute value. They do, however, agree very well

Table 2: Temperature Dependence Studies for Surface Variants of Glucose Oxidase

enzyme	data set	$A_D/A_{T(\text{full } T \text{ range})}$[a]	$A_D/A_{T(\text{int. est.})}$[a,b]	$\Delta H^{\ddagger}(k_{cat}/K_M,T)$[c]	$\Delta H^{\ddagger}(k_{cat},D)$[c]	T_M (pH 8.3)[d]	T_M (pH 7.5)[d]
WT GO	present study	0.98 ± 0.18	0.98 ± 0.18	5.5 ± 0.9	11.5 ± 0.3	44.9 ± 1.1	58.5 ± 1.0
	40	0.97 ± 0.07	0.97 ± 0.07				
	1	1.25 ± 0.04	1.25 ± 0.04				
Degly320 GO	present study	0.90 ± 0.05	0.81 ± 0.08	5.0 ± 0.4	11.1 ± 0.3	47.8 ± 1.0	58.3 ± 1.1
Degly205 GO	*1*	1.13 ± 0.05	1.04 ± 0.08				
Rec320 GO	present study	0.83 ± 0.05	0.62 ± 0.07	4.4 ± 0.6	10.9 ± 0.3	48.8 ± 0.8	59.4 ± 1.3
Rec205	*40*	0.63 ± 0.05	0.57 ± 0.06				
Rec205	*1*	0.89 ± 0.04	0.81 ± 0.08				
PEG-5000 GO	present study	0.73 ± 0.04	0.55 ± 0.05	4.1 ± 0.3	10.8 ± 0.3	48.5 ± 0.8	60.2 ± 1.1
PEG-350 GO	present study	0.76 ± 0.04	0.55 ± 0.05	4.8 ± 0.6	11.3 ± 0.3	43.4 ± 0.9	56.5 ± 2.3

[a] Based on D/T KIE data corrected for protium contamination as appropriate. [b] As described in the text, the best estimate of the intrinsic value of A_D/A_T based on interpretation of the change in kinetic complexity for the particular enzyme. For all but WT GO, data from 15 to 50 °C were used. The full temperature range was used for WT GO. [c] Enthalpies of activation are reported in kilocalories per mole, where T refers to C−T cleavage and D refers to C−D cleavage. [d] The thermal melting temperature is reported in degrees Celsius, and the pH that is reported was measured at 40 °C.

with the trend among the three glycoforms. We tentatively attribute the upward shifting of values for A_D/A_T in Kohen et al. (*1*) to a difference between the solute-to-scintillant ratio used in experiments versus the calibration curve for the scintillation counter (*42*).

Correlation between A_D/A_T and Enthalpy of Activation on k_{cat}/K_M. To understand better the differences in A_D/A_T caused by variations at the surface of GO, we looked for correlations with other catalytic and physical parameters. Examination of the temperature dependence for k_{cat}/K_M allows direct comparison with the H/T and D/T KIEs, which are a measure of k_{cat}/K_M ratios for the light versus heavy isotope. As presented in Methods and derived in the Appendix, it is possible to extract k_{cat}/K_M rate constants from the competitive KIE experiments. This becomes particularly important for the tritiated substrates, which are generally unavailable by other means. In this method, the fractional conversion of each isotope is plotted versus time for each experiment performed. The data are then fitted to the appropriate equation to give the rate at time zero, the initial velocity. At higher temperatures, it was found that the reaction did not go to complete conversion due to inactivation of the enzyme over the several hour duration of the experiment. Nonetheless, the apparent first-order rate constant, which is equal to the initial enzyme concentration times k_{cat}/K_M, could be determined by assuming the inactivation of the enzyme was a first-order process (eq 3). A comparison of k_{cat}/K_M measured for [1-^{1}H]-2-deoxyglucose using this new method, versus the value determined via oxygen uptake kinetics, is shown in Figure 3, demonstrating that the method works quite well. Note that for this method to be applied, the amount of substrate in an E·S complex must be very small relative to the total enzyme concentration (although this is not required to obtain a KIE on k_{cat}/K_M). The advantages of this method are (i) that competitive KIE experiments can be used to monitor simultaneously rate and KIE data, with only subtle modification of the design of the experiments, and (ii) that k_{cat}/K_M can be assessed for the tritiated substrate. This substrate, having the slowest rate among the three hydrogen isotopes, will be the least masked by kinetic complexity. Therefore, differences in its temperature dependence among a series of modified enzymes will report most clearly on differences in the behavior of the chemical step. Table 2 lists the $\Delta H^{\ddagger}$ determined for each enzyme form with [1-^{3}H]-2-deoxyglucose as a substrate.

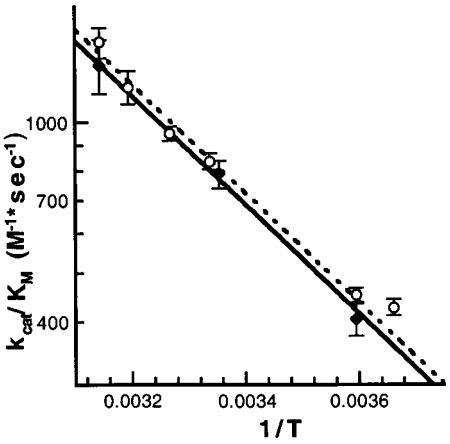

FIGURE 3: Validation of the method: k_{cat}/K_M for [1-^{1}H]-2-deoxyglucose for Degly GO extracted from competitive KIE experiments (○) vs measurement by oxygen uptake (◆).

Figure 4A examines the correlation between this $\Delta H^{\ddagger}(k_{cat}/K_M,T)$ and A_D/A_T. Although the differences in the enthalpy of activation are quite small, and the error bars are large, a correlation R of 0.998 is found in a linear fit to all the enzymes except the PEG-350 GO.

Correlation between A_D/A_T and the Enthalpy of Activation on k_{cat}. The enthalpies of activation were also measured on k_{cat} using [1-^{2}H]-2-deoxyglucose and each of the available enzyme forms (Table 2). A possible significance of these data was initially disregarded, as it was found that the large differences among the enzyme forms reported in Kohen et al. (*1*) were due to a mixing artifact,[2] with experimental trends being much smaller. However, after finding small differences among the enzyme forms in the $\Delta H^{\ddagger}$ for k_{cat}/K_M and an apparent correlation of $\Delta H^{\ddagger}$ to A_D/A_T, we proceeded to examine whether a similar trend would be present in $\Delta H^{\ddagger}$

[2] There is an initial artificial burst in the rate when injecting a sample at an ≈5-fold lower air oxygen concentration into an oxygen-saturated solution. The amplitude of this burst is proportional to the volume of the injection. The stock solutions of the three enzymes in the previous study were at different concentrations, and thus, systematically different volumes were injected in kinetics runs. This resulted in an artificial separation of the rates among the three enzyme forms at low temperatures, where the real rates were unfortunately on the same order as the magnitude of this burst. Remeasurement of the exact enzymes used in that study found the differences in the rates to be very small at both low and high temperatures. We have taken great care to avoid this problem in the present study.

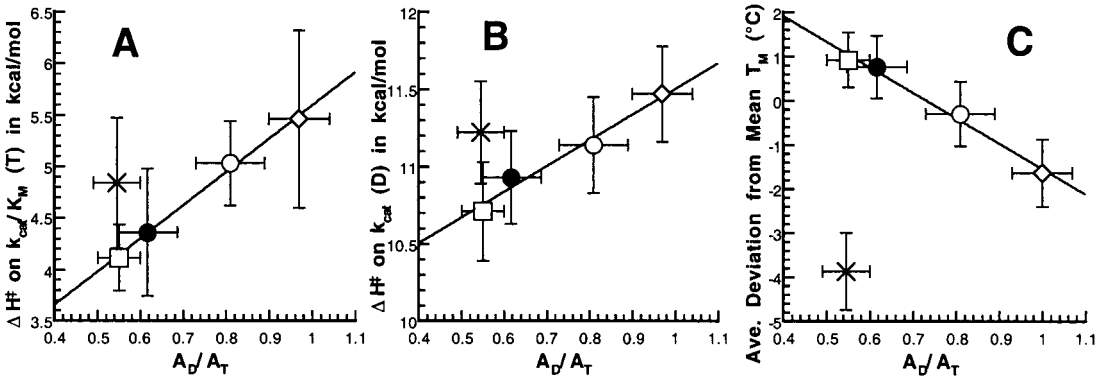

FIGURE 4: Correlation analyses among measured parameters. Fittings are weighted linear fits for all enzymes except PEG-350 GO: WT GO (◇), Degly GO (○), Rec GO (●), PEG-350 GO (×), and PEG-5000 GO (□). (A) $\Delta H^{\ddagger}$ on k_{cat}/K_M for [1-^{3}H]-2-deoxyglucose vs A_D/A_T. (B) $\Delta H^{\ddagger}$ on k_{cat} for [1-^{2}H]-2-deoxyglucose vs A_D/A_T. (C) Average deviation from the mean T_M vs A_D/A_T. The points are the averages of the deviation from the respective mean T_M at each pH, as reported in Table 2. The mean T_M data are for the four correlating enzyme variants and do not include the value for PEG-350 GO.

for k_{cat}. As shown in Figure 4B, the enthalpy of activation for k_{cat} also shows a correlation to A_D/A_T ($R = 0.985$) for WT GO, Degly320 GO, Rec320 GO, and PE-5000 GO; once again, the results for PEG-350 GO are off the line. The fact that we see similar trends in panels A and B of Figure 4 suggests that these observations reflect a functionally relevant property of the modified enzymes.

To quantify the extent to which the trends in $\Delta H^{\ddagger}$ observed for the two independently determined k_{cat} versus k_{cat}/K_m parameters are similar, we analyzed the linear correlation between the two parameters for all five enzyme forms and found an R of 0.939 (data not shown). The high correlation despite the inclusion of PEG-350 GO means that this form is consistently aberrant in panels A and B of Figure 4. Since the chemical step is the only microscopic rate constant found in both k_{cat}/K_M and k_{cat} [assuming the chemical step is irreversible (*31*)], and because the chemical step dominates both of these parameters as evidenced by the large KIEs, we conclude that there are quite small but likely significant differences in the enthalpy of activation for C−H bond cleavage (k_2) among the enzyme forms. Differential stability of the enzyme forms is an unlikely source of the observed trends, because the k_{cat} measurements are initial velocities while the k_{cat}/K_M values are conducted over longer time periods. Additionally, data near the T_M (see below) have been excluded.

Correlation between A_D/A_T and Thermal Melting Temperature. The apparent thermal melting temperature was measured at two different pH values for each of the enzyme forms. The unfolding was found to be irreversible, as expected for an enzyme the size of GO. Nonetheless, these data show a very similar trend among the four enzyme variants for which $\Delta H^{\ddagger}$ and A_D/A_T are found to correlate. The correlation of T_M and A_D/A_T is very similar at pH 7.5 and 8.3 (Table 2). To illustrate the correlation of the T_M to A_D/A_T at different pHs, we have taken the mean of the four enzymes (excluding PEG-350 GO) that correlate well at each pH and then averaged the deviation from the respective mean for each enzyme. Figure 4C shows a plot of these average deviations from the mean T_M; a weighted linear fitting to the data gives a correlation R of 0.993. The data for PEG-350 GO have been included in the graph to show the consistency of their deviation from the remaining enzyme forms for the three determinations summarized in panels A−C of Figure 4.

DISCUSSION

Effects of Surface Modifications on GO. A previous study of the temperature dependence of KIEs with GO found an unexpected difference between WT GO and Rec205 GO (*56*). This prompted the preparation and characterization of Degly205 GO, and the proposal of a role for surface changes in modulating active site hydrogen tunneling. In the work of Kohen et al. (*1*), the trend in A_D/A_T observed among the glycoforms of GO suggested that the changes in this catalytic parameter were correlated to the overall mass of protein. However, with the benefit of the additional data and analyses presented herein (Table 2), it is clear that simple mass effects will not suffice to explain the observed effects. The general picture that emerges is that the WT and Degly GO have an A_D/A_T near to unity, and that all heavily glycosylated or PEGylated surface variants have A_D/A_T values below unity. Assuming the "perfecting power" of evolutionary pressure, we postulate that the surface environment of the WT protein is likely to be the most optimal for catalysis. In this context, the deviation of the properties (e.g., A_D/A_T) for surface-modified variants of GO is proposed to reflect the extent to which the surface environment is altered from that of the WT.

This hypothesis can be examined with Table 1, which summarizes the number of modified sites and the average size of the group attached at each site for the GO variants. WT GO has rather small polysaccharide chains, the average length being ~10 sugars, and is the reference surface environment. Upon removal of most of these sugars in Degly GO, approximately two sugars remain per attachment point. As the first few sugars are believed to be the ones most strongly interacting with the protein (*57*), conversion of WT GO to Degly GO is not a drastic change. Both Rec205 GO and Rec320 GO have enormous polysaccharide chains compared to the WT protein (4 and 10 times the size, respectively). Both recombinant proteins may exceed some threshold such that their polysaccharide chains are large enough to have substantial interaction with the surface of the protein or with other sugar branches. This may explain their almost indistinguishable behavior. The surface of both

PEG proteins can also be viewed as being far more different from the WT GO than Degly GO, which is the starting point for the addition of the polyether. The fact that PEG has less hydrogen bonding capacity than water or sugar is expected to increase the divergence of the surface environment of PEGylated proteins from the WT. Additionally, linkage of PEG to protein converts positively charged lysines to uncharged amide linkages. It is significant that T_M correlates with changes in A_D/A_T (Figure 4C). Although the T_Ms are not reversible and do not, therefore, measure thermodynamic parameters, the trend in T_M reflects the different kinetic susceptibility to denaturation. Since the only changes among the GO variants are at the surface, these data can be taken as evidence that surface perturbations are altering a physicochemical aspect of the protein, which causes proportionate changes in the catalytic parameter, A_D/A_T. The PEG-350 GO does not fit this correlation, nor does it fit the correlations to the measured enthalpies of activation, as shown in panes A and B of Figure 4. This is likely to be rooted in the fact that this variant has far more modifying groups attached to its surface than the other protein variants (Table 1), due to greater steric access of the smaller PEG reagent. The extent of labeling of PEG-350 GO may "lever" open the protein, affecting the polypeptide structure in such a way as to impact both $\Delta H^{\ddagger}$ and T_M.

An uncertainty is how changes at the protein surface are transmitted to the active site of GO. One possible mechanism of transmission is a subtle alteration in the static structure of the enzyme. This must be a very small change because the k_{cat} values at 33 °C (Table 1) are almost unchanged. A second mechanism for the transmission of changes at the surface to the active site is an alteration of conformational dynamical motions that span a substantial part of the protein and contribute to the reaction coordinate. Both the PEG and polysaccharide act as viscosogens that behave at an exceedingly high effective concentration on the surface of the protein. Altering the surface environment from that of the WT may misalign the evolutionarily refined motions; i.e., the altered "microviscosity" on the surface may act as a frictional drag, affecting rates of hydrogen transfer in an isotope-dependent manner. The transmission of motion from the surface may arise from slower, large-scale motions that affect faster motions at the active site. Descriptions with two environmental coordinates have been presented by Bialek and Onuchic (*58*), Ulstrup and co-workers (*59*), and Borgis and Hynes (*15*, *18*).

The key observation in this study is the trend in A_D/A_T among the enzymes (WT GO $\cong$ Degly GO > Rec GO > PEG-5000 GO), which we ascribe to an increasing level of deviation of the environment at the enzyme surface from that of the optimized WT protein. As will be discussed below, two other enzymatic systems have been described (a thermophilic alcohol dehydrogenase and soybean lipoxygenase) where deviation from WT protein causes the temperature dependence of KIEs to yield a decreased isotope effect on the Arrhenius prefactor (*3*, *33*).

Theories of Hydrogen Tunneling. Numerous reports of the occurrence of hydrogen tunneling in enzymatic reactions have been based on the observation of behaviors that are inconsistent with the "semiclassical"[3] theory of isotope effects, a version of classical transition state theory (TST) that takes into account the quantum feature of isotopic zero-point energy differences (*60*). Much of the early evidence for tunneling in enzymes came from nonclassical relations between H/T and D/T KIEs, termed deviations from the Swain-Schaad relationship, which states $(k_D/k_T)^{3.3} = k_H/k_T$ in the absence of tunneling (*3*, *54*, *61*, *62*). Other reports have been focused on deviations from the expected temperature dependence of KIEs, in particular, the failure to observe the predicted KIE of close to unity on the Arrhenius prefactor (*3*, *33*, *63*) [with a lower semiclassical limit of 0.6 for H/T KIEs and 0.9 for D/T KIEs (*64*, *65*)]. All of these deviations from expected behavior were originally rationalized by adding a correction for tunneling to TST (*66*).

Based on a semiclassical view of KIEs that allows for a tunneling correction, plots of the temperature dependence of the KIE have been divided into four regions of phenomenological behavior that differ in the degree of tunneling (*2*, *67*). When we start at the high-temperature limit, the KIE in the Arrhenius prefactor is the semiclassically predicted value of unity. When we move toward lower temperatures and the onset of a tunneling contribution for the lighter isotope, the KIE on the Arrhenius prefactor can go significantly below one. It then "recovers" and becomes greater than unity, as the tunneling contribution to the transfer of the heavy isotope becomes substantial. Finally, at the extreme limit of low temperatures, tunneling dominates for both isotopes, and the KIE becomes independent of temperature. It was in the context of such a picture that the original data on GO (*1*) were interpreted.

Modern theories of hydrogen transfer are much closer to the Marcus theory for electron transfer (*68*). Beginning with the work of Dogonadze, Levich, and Kuznetsov (*69*), we can view the energetic barrier to the hydrogen transfer as arising from heavy atom rearrangements that achieve the requisite degeneracy between the donor and acceptor hydrogen wave functions for tunneling to occur. In this picture, the hydrogen movement is always quantum mechanical and occurs along a separate reaction coordinate from the heavy atoms. One feature that clearly distinguishes hydrogen from electron tunneling is the much larger mass of the former. This has led to the incorporation of an additional term for hydrogen ransfer, the distance dependence between the donor and acceptor heavy atoms. Johnson and Rapp (*70*) first suggested the importance of integrating over various possible distances to the rate of hydrogen transfer (as discussed in ref *19*). There are now many theoretical treatments that include this feature (*13*, *15*, *17*−*25*).

In the context of the present work, it is important to consider the expected temperature dependencies of hydrogen KIEs for full tunneling models. Such a treatment has been published recently by Kuznetsov and Ulstrup (*25*) and is most straightforward in the nonadiabatic limit when there is little coupling between the donor and the acceptor wave functions. According to their treatment, two temperature-dependent terms can modulate tunneling. The first of these terms reflects the heavy atom reorganization that matches the energies of reactant and product wells and which is largely isotope

[3] The term "semiclassical" unfortunately is used two different ways with opposite implications. Here we use it to mean a classical view that includes the one quantum feature of zero-point energy differences but no tunneling. The more common usage of the term refers to a type of approximation for a tunneling reaction.

independent. In the absence of additional factors, the isotope effect comes from the nuclear overlap term, which is close to temperature independent. This leads to isotope effects that change relatively little with temperature and produce values for A_1/A_2 larger than unity.

A more sophisticated model is one in which the distance between the donor and acceptor changes (gating). The actual transfer distance is a compromise between the increased probability for tunneling at reduced distances and the energetic cost of achieving the reduced distance. Two significant features of this model are that (i) the actual transfer distance is different for the light and heavy isotope effect ($r_D < r_H$), and, consequently, (ii) $\Delta G_D^{\ddagger} > \Delta G_H^{\ddagger}$. Depending on the importance of gating to the hydrogen transfer, the isotope effect on the Arrhenius prefactor can be reduced to unity, and then further reduced to values significantly less than unity as gating predominates (*23*−*25*, *33*).

Trends in Isotope Effects on the Arrhenius Prefactor for Thermophilic Alcohol Dehydrogenase and Lipoxygenase. Previously published examples of isotope effects on the Arrhenius prefactor that decrease as a protein is modified away from a nativelike structure are found with the thermophilic alcohol dehydrogenase (TADH) (*3*) and soybean lipoxygenase (SLO) (*33*). The WT SLO reaction is rare among enzyme-catalyzed C−H cleavage processes in that the observed hydrogen and deuterium transfer rates are close to temperature independent and the isotope effects are huge (in the range of 100 at room temperature). This hydrogen atom transfer reaction is probably the best example of a pure tunneling process within an enzyme-catalyzed reaction. Recent modeling of the WT form of SLO indicates that the data can be fit by a sizable environmental reorganization term, together with a frequency for gating that is high ($\omega_g = 400$ cm^{-1}) in relation to room temperature ($k_T \cong 200$ cm^{-1}). This behavior has been interpreted in terms of a tightly packed enzyme active site where the configuration of the bound substrate is controlled by numerous hydrophobic side chains. Mutation of hydrophobic side chains within this active site has the effect of decreasing A_D/A_T. Modeling of the mutant data shows a trend of decreasing gating frequency, indicative of increased protein flexibility and a greater contribution of protein gating to hydrogen transfer (*33*).

In the case of the TADH, two regions of temperature-dependent behavior have been identified, one at elevated temperatures near the physiologically relevant temperature and one at reduced temperatures, where the rate of enzymatic turnover falls off. This system shows the paradoxical behavior of tunneling at elevated temperatures, attributed to a role for dynamics in the efficient barrier penetration by hydrogen. In this instance, an important tool for assessing tunneling was the magnitude of the exponent relating the secondary H/T and D/T isotope effects (*3*), which was found to be more deviant from classical behavior at high than low temperatures.

Examination of noncompetitive KIEs also indicated a pattern where $A_H/A_D > 1$ in the region of optimal temperature, which changed to $A_H/A_D < 1$ at reduced temperatures. If we were to apply the full quantum model of Kuznetsov and Ulstrup to explain the pattern of the temperature dependence of the KIEs with TADH, we would conclude that there is less dependence on gating modes when the protein is optimal and flexible ($A_H/A_D > 1$) and that reduction in temperature, with its concomitant stiffening, introduces the need for a specific gating mode(s) ($A_H/A_D < 1$). However, the decreasing magnitude of the exponent relating secondary D/T and H/T isotope effects with decreasing temperature is opposite to that predicted by Krishtalik (*23*), who estimates that an increased level of gating will elevate the primary exponent relating the D/T and H/T isotope effects.

Thus, with the theories in hand, it is not possible to explain the trends in both competitive and noncompetitive KIEs for TADH within a full tunneling model and different degrees of dynamical gating. Since there is a clear correlation between protein flexibility and tunneling, it is also not possible to apply fully static models for tunneling to interpret the observed trends in behavior. It is for this reason that the data are best viewed in the context of close to full tunneling behavior at elevated temperatures, which is the physiological range of enzyme activity. A reduction in temperature compromises the ability of the protein to create the same reaction coordinate, and the proton must now "mount" a more classical barrier, with the attendant increase in the observed energy of activation for both H and D. The inverse isotope effect on the Arrhenius prefactor would then result from the greater ease of tunneling beneath the classical barrier for the lighter isotope.

Origin of the Relation $A_D/A_T < 1$ with Surface-Modified GO. Analogous to SLO and TADH, GO shows an isotope effect on the Arrhenius prefactor that becomes more inverse as the behavior of the protein moves away from its optimal state. One possible interpretation for this behavior is in the context of SLO. In this model, the modification of the outer envelope of GO would have its impact on the initial distance between the donor and acceptor atoms involved in hydrogen transfer at the active site. The WT protein is viewed as being optimal, requiring some gating to achieve the correct distance for efficient tunneling and to bring the isotope effect on the Arrhenius prefactor below the observed values for the isotope effects. Changes in the envelope of the protein shift the achievable distance between the donor and acceptor atoms to a small extent, reflecting a propagation of structural effects from the outer surface of the protein to the active site. This change in positioning is best tolerated for protium, with its longest wavelength and greater capacity to tunnel over long distances. The isotopes D and T are no longer capable of efficient tunneling and must undergo a greater degree of gating than protium, with the gating in the following order: T > D > H. This produces a larger energy of activation for T than for D and the observed trend in decreasing A_D/A_T for protein variants. A difficulty that arises in applying this tunneling interpretation to GO is that gating leads, in general, to an increase in the energy of activation of the reaction. In contrast, the experimental data in Figure 4 indicate that deviation of A_D/A_T from unity is accompanied by very small changes or decreases in $\Delta H^{\ddagger}$.

In analogy to TADH, an alternate view is that GO undergoes a transition in the properties of its reaction coordinate as the protein surface is modified, e.g., via stiffening, as suggested by the increased T_M for the protein that is either extensively glycosylated or modified with PEG-5000. In the WT enzyme, dynamical motions lead to sampling among different ground state geometries with varying distances between reactant and product energy wells. As the

distance between the donor and acceptor is reduced, the height of the hydrogen transfer barrier is also reduced, creating a state that allows a close to over the barrier, adiabatic hydrogen transfer. When the motions that permit sampling of multiple ground state geometries are modified in response to protein surface changes, the reduction in barrier height that accompanies ground state sampling may become more difficult to achieve. The transferred hydrogen encounters an elevated C−H barrier through which it is now forced to tunnel (*71*). The very small decreases in the enthalpy of activation for all isotopes may reflect a balance between the increased height of the barrier and the decreased enthalpy of activation that accompanies an increased level of tunneling. In this instance, the inverse isotope effect on the Arrhenius prefactor reflects the greater ease for the lighter isotope to move under the barrier. Note that while this explanation is similar to that for TADH, the hydrogen transfer for WT GO is closest to classical behavior, only moving into a more tunneling-like regime when protein dynamical modes are altered as a result of extensive surface modification.

CONCLUSIONS

Surface-modified glucose oxidases, containing varying degrees of glycosylation or PEGylation, display similar alterations in the temperature dependence of kinetic isotope effects. Unexpectedly, the observed changes in kinetic behavior for hydrogen transfer are independent of either the mass or chemical nature of the group appended to the protein surface. We conclude that deviations in the structure of the protein−solvent interface from that in native protein impact subtle but essential interactions of protein dynamical motions with the chemical reaction coordinate. The quantum nature of hydrogen transfer and its resulting sensitivity to heavy atom motions provide a sensitive probe for the interaction of distal protein structural changes on active site chemistry.

ACKNOWLEDGMENT

We thank Dr. Steven Rosenberg (formerly of Chiron Co.) for the generous gift of both the recombinant protein and the yeast expression system. We thank Liza Levina and Jean Yang of the Department of Statistics, University of California, Berkeley, for their help in determining the most appropriate methods for data analysis and statistics and Dimitri Curtil of Lawrence Berkeley National Laboratory (Berkeley, CA) for his valuable mathematical assistance. We acknowledge Prof. Jack Kirsch and Prof. Susan Marqusee of the Department of Molecular and Cell Biology, University of California, Berkeley, for access and assistance with instrumentation in their laboratories. Finally, we thank Prof. Amnon Kohen (currently at the University of Iowa, Iowa City, IA) for the preparation of the recombinant GO used in this study and for many valuable discussions and assistance, and Prof. Thorlakur Jonsson (DeCode Genetics, Inc., Reykjavik, Iceland), who initiated studies on GO in this laboratory and laid the foundation for the work presented herein.

SUPPORTING INFORMATION AVAILABLE

Synthesis of [1-^{2}H]-2-deoxyglucose and kinetic parameters for several glucose oxidases. This material is available free of charge via the Internet at http://pubs.acs.org.

APPENDIX

Derivation of eq 3 in the Text. Here we present the derivation and validation of the equation used to fit fractional conversion versus time from competitive KIE experiments. The goal of the fitting is to extract the k_{cat}/K_M values from these data for the individual isotopes. By analysis of experiments over a range of temperatures, the enthalpy of activation can be obtained for any of the isotopically labeled substrates, including tritium. Although irreversible inactivation of the enzyme has no influence on the ratio of isotopic rate constants (the KIE), it will influence the apparent rate constants (k_{cat}/K_M) of the separate isotopes. Thus, this inactivation must be taken into account to arrive at the correct values of k_{cat}/K_M. The presence of inactivation was clearly evidenced at higher temperatures by the failure to attain complete conversion of the substrate to product at infinite time.

We begin by noting that enzyme and substrate concentrations typically used in the competitive KIE experiments reported in this paper were as follows: ≈0.25 μM enzyme, ≈1.3 μM [1-^{1}H]-2-deoxyglucose, ≈4.7 μM [1-^{2}H]-2-deoxyglucose, and ≈0.0044 μM [1-^{3}H]-2-deoxyglucose in H/T KIE experiments and ≈0.028 μM [1-^{3}H]-2-deoxyglucose in D/T KIE experiments. The highest sugar substrate concentrations were at least 3 orders of magnitude below the lowest K_M measured for that substrate (≈17 mM at 5 °C). In all the experiments, the oxygen concentration was at least 200 μM and effectively constant throughout the reaction since the sugar is the limiting reagent. The measured K_M value for oxygen as a function of temperature with saturating substrate ranged from 20 to 300 μM; however, according to eq 2 in the paper, the apparent K_M for O_2 at low sugar concentrations will be far smaller than these values. Therefore, all experiments occur in the O_2-saturated regime, as well as far below the K_M for sugar, and we can assume the second half-reaction in Scheme 1 is always extremely fast compared to the first half-reaction. An equation for the first half-reaction that allows for inactivation of the enzyme is given below:

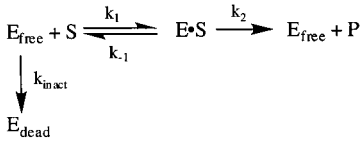

(A-1)

where S is the substrate, E_{free} is the active free form of the enzyme, E·S is the substrate-bound enzyme complex, E_{dead} is the inactivated enzyme, and P is the product. The rate, d[S]/dt, as a function of time will then be described by

$$\frac{d[S]}{dt} = -k[S][E_{free}] \qquad \text{(A-2)}$$

where k is the second-order rate constant. In the event that the substrate concentration at time zero were in the saturating regime, $[E_{free}]$ would be low at early times and increase throughout the time course. Derivation of an expression for the change in [P] with time in this situation, while allowing for k_{inact}, would be very difficult and would necessitate solving a series of differential equations. However, since the highest substrate concentration at time zero is well below K_M, we can assume that [E·S] is effectively zero at all times,

i.e., that enzyme exists only in two forms: the active, free enzyme, E_{free}, and the inactive enzyme, E_{dead}. Similarly, we can assume that the initial concentration of S, $[S]_0$, is effectively partitioned into either S or P at some time, t, and allows us to assume $d[S]/dt = -d[P]/dt$. Under these conditions, the partitioning of the initial concentration of the enzyme ($[E]_0$) between E_{free} and E_{dead} is independent of the substrate concentration. We can, therefore, describe the change in $[E_{free}]$ as a function of time with a simple exponential decay from the initial value at time zero:

$$[E_{free}] = [E_0]e^{-k_{inact}t} \qquad \text{(A-3)}$$

Substituting this into eq A-2, we have

$$\frac{d[S]}{dt} = -k[S][E_0]e^{-k_{inact}t} \qquad \text{(A-4)}$$

The expression for the rate at time zero is $(k_{cat}/K_M)[E_0][S]$. If we lump the constant terms, $[E_0]$, and k_{cat}/K_M into one constant, k_{rate}, we obtain eq A-5:

$$\frac{d[S]}{dt} = -k_{rate}[S]e^{-k_{inact}t} \qquad \text{(A-5)}$$

An expression for the change in product as a function of time can now be obtained by solving the differential equation with separable variables:

$$\int_{[S]_0}^{[S]_t}\frac{1}{[S]}d[S] = -k_{rate}\int_0^t e^{-k_{inact}t}\,dt \qquad \text{(A-6)}$$

Integration gives the general solution

$$\ln\left(\frac{[S]_t}{[S]_0}\right) = -\frac{k_{rate}}{k_{inact}}(1 - e^{-k_{inact}t}) + C \qquad \text{(A-7)}$$

Solving for the integration constant, C, with the initial condition that $[S]/[S]_0 = 1$ when $t = 0$ yields $C = 0$. The specific solution, after taking the inverse natural log of both sides, is

$$\frac{[S(t)]}{[S_0]} = e^{-\left(\frac{k_{rate}}{k_{inact}}\right)\left(1-e^{-k_{inact}t}\right)} \qquad \text{(A-8)}$$

As noted earlier, the amount of S in E·S is effectively zero such that the rate of disappearance of S equals the rate of appearance of the product. Fractional conversion at time t can then be related to the fraction of substrate remaining by

$$f(t) = \frac{[P]_t}{[S]_0} = 1 - \frac{[S]_t}{[S]_0} \qquad \text{(A-9)}$$

Substituting our function for $[S]_t/[S]_0$ into eq A-8 leads to the expression for fraternal conversion versus time with allowance for enzyme inactivation:

$$f(t) = 1 - e^{-\left(\frac{k_{rate}}{k_{inact}}\right)\left(1-e^{-k_{inact}t}\right)} \qquad \text{(A-10)}$$

It is important to note that although this equation appears to suffer a division by zero in the limit of $k_{inact} = 0$, the numerator in the exponent goes to zero more rapidly than the denominator, leading to eq A-11 in the absence of any inactivation of enzyme

$$\lim_{k_{inact}\to 0} f(t) = 1 - e^{-k_{rate}t} \qquad \text{(A-11)}$$

REFERENCES

1. Kohen, A., Jonsson, T., and Klinman, J. P. (1997) *Biochemistry 36*, 2603−2611.
2. Kohen, A., and Klinman, J. P. (1998) *Acc. Chem. Res. 31*, 397−404.
3. Kohen, A., Cannio, R., Bartolucci, S., and Klinman, J. P. (1999) *Nature 399*, 496−499.
4. Fleming, G. R. (1998) *Proc. Natl. Acad. Sci. U.S.A. 95*, 15161−15162.
5. Jordanides, X. J., Lang, M. J., Song, X. Y., and Fleming, G. R. (1999) *J. Phys. Chem. B 103*, 7995−8005.
6. Lim, M. H., Hamm, P., and Hochstrasser, R. M. (1998) *Proc. Natl. Acad. Sci. U.S.A. 95*, 15315−15320.
7. Weiss, S. (1999) *Science 283*, 1676−1683.
8. Xie, X. S., and Lu, H. P. (1999) *J. Biol. Chem. 274*, 15967−15970.
9. Fitter, J. (1999) *Biophys. J. 76*, 1034−1042.
10. Zaccai, G. (2000) *Science 288*, 1604−1607.
11. Schlichting, I., Berendzen, J., Chu, K., Stock, A. M., Maves, S. A., Benson, D. E., Sweet, B. M., Ringe, D., Petsko, G. A., and Sligar, S. G. (2000) *Science 287*, 1615−1622.
12. Lu, H. P., Xun, L. Y., and Xie, X. S. (1998) *Science 282*, 1877−1882.
13. Antoniou, D., and Schwartz, S. D. (1997) *Proc. Natl. Acad. Sci. U.S.A. 94*, 12360−12365.
14. Antoniou, D., and Schwartz, S. D. (1998) *J. Chem. Phys. 108*, 3620−3625.
15. Borgis, D., Lee, S. Y., and Hynes, J. T. (1989) *Chem. Phys. Lett. 162*, 19−26.
16. Borgis, D., and Hynes, J. T. (1989) in *The Enzyme Catalysis Process: Energetics, Mechanism, and Dynamics* (Cooper, A., Houben, J. L., and Chien, L. C., Eds.) Plenum Press, New York.
17. Borgis, D., and Hynes, J. T. (1993) *Chem. Phys. 170*, 315−346.
18. Borgis, D., and Hynes, J. T. (1996) *J. Phys. Chem. 100*, 1118−1128.
19. Bruno, W. J. (1990) Ph.D. Thesis, University of California, Berkeley, CA.
20. Bruno, W. J., and Bialek, W. (1992) *Biophys. J. 63*, 689−699.
21. Suárez, A., and Sibley, R. (1991) *J. Chem. Phys. 94*, 4809−4816.
22. Sumi, H., and Ulstrup, J. (1988) *Biochim. Biophys. Acta 955*, 26−42.
23. Krishtalik, L. I. (2000) *Biochim. Biophys. Acta 1458*, 6−27.
24. Kuznetsov, A. M., and Ulstrup, J. (1994) *Chem. Phys. 188*, 131−141.
25. Kuznetsov, A. M., and Ulstrup, J. (1999) *Can. J. Chem. 77*, 1085−1096.
26. Hwang, J. K., and Warshel, A. (1996) *J. Am. Chem. Soc. 118*, 11745−11751.
27. Swain, C. G., Stivers, E. C., Reuwer, J. F., Jr., and Schaad, L. J. (1958) *J. Am. Chem. Soc. 80*, 5885−5893.
28. Bahnson, B. J., and Klinman, J. P. (1995) *Methods Enzymol. 249*, 373−397.
29. Dahlquist, F. W., Rand-Meir, T., and Raftery, M. A. (1969) *Biochemistry 8*, 4214−4221.
30. Kohen, A., Jonsson, T., and Klinman, J. P. (1997) *Biochemistry 36*, 6854−6854.
31. Gibson, H. Q., Swoboda, B. E. P., and Massey, V. (1964) *J. Biol. Chem. 239*, 3927−3934.
32. Nakamura, S., and Ogura, Y. (1968) *J. Biochem. 63*, 308−316.
33. Knapp, M. J., Rickert, K., and Klinman, J. P. (2002) *J. Am. Chem. Soc. 124*, 3865−3874.

34. Frederick, K. R., Tung, J., Emerick, R. S., Masiarz, F. R., Chamberlain, S. H., Vasavada, A., and Rosenberg, S. (1990) *J. Biol. Chem. 265*, 3793−3802.
35. Isbell, H. S. (1932) *Bur. Stand. J. Res. 8*, 615−624.
36. Wolfrom, M. L., and Wood, W. G. (1951) *J. Am. Chem. Soc. 73*, 2933−2934.
37. Stocks, S. J., Jones, A. J. M., Ramey, C., and Brooks, D. E. (1986) *Anal. Biochem. 154*, 232−234.
38. Lai, C. Y. (1977) *Methods Enzymol. 47*, 236−243.
39. Karr, L. J., Donnelly, D. L., Kozlowski, A., and Harris, J. M. (1994) *Methods Enzymol. 228*, 377−390.
40. Grant, K. L., and Klinman, J. P. (1989) *Biochemistry 28*, 6597−6605.
41. Rucker, J., Cha, Y., Jonsson, T., Grant, K. L., and Klinman, J. P. (1992) *Biochemistry 31*, 11489−11499.
42. Seymour, S. L. (2001) The Influence of Enzyme Surface and Environmental Modifications on Catalysis Examined with Probes for Hydrogen Tunneling, Ph.D. Thesis, University of California, Berkeley, CA.
43. Department of Statistics, Consulting Center (2001) University of California, Berkeley, CA.
44. Segel, I. H. (1993) *Enzyme Kinetics*, Wiley, New York.
45. Hollien, J., and Marqusee, S. (1999) *Biochemistry 38*, 3831−3836.
46. McGoff, P., Baziotis, A. C., and Maskiewicz, R. (1988) *Chem. Pharm. Bull. 36*, 3079−3091.
47. Grant, K. L., and Klinman, J. P. (1992) *Bioorg. Chem. 20*, 1−7.
48. Jonsson, T., Edmondson, D. E., and Klinman, J. P. (1994) *Biochemistry 33*, 14871−14878.
49. Cornish-Bowden, A. (1995) *Analysis of Enzyme Kinetic Data*, Oxford University Press, New York.
50. Cleland, W. W. (1978) *Adv. Enzymol. 45*, 273−387.
51. Northrop, D. B. (1981) *Annu. Rev. Biochem. 50*, 103−131.
52. Cha, Y., Murray, C. J., and Klinman, J. P. (1989) *Science 243*, 1325−1330.
53. Bahnson, B. J., Colby, T. D., Chin, J. K., Goldstein, B. M., and Klinman, J. P. (1997) *Proc. Natl. Acad. Sci. U.S.A. 94*, 12797−12802.
54. Chin, J. K., and Klinman, J. P. (2000) *Biochemistry 39*, 1278−1284.
55. Bright, H. J., and Gibson, H. Q. (1966) *J. Biol. Chem. 242*, 994−1003.
56. Jonsson, T. (1995) Probes of Hydrogen Tunneling in Enzymes, Ph.D. Thesis, University of California, Berkeley, CA.
57. Live, D. H., Williams, L. J., Kuduk, S. D., Schwartz, J. B., Glunz, P. W., Chen, Z., Sames, D., Kumar, R. A., and Danishefsky, S. J. (1999) *Proc. Natl. Acad. Sci. U.S.A. 96*, 3489−3493.
58. Bialek, W., and Onuchic, J. N. (1988) *Proc. Natl. Acad. Sci. U.S.A. 85*, 5908−5912.
59. Goguadze, N. G., Hammerstad-Pedersen, J. M., Khoshtariya, D. E., and Ulstrup, J. (1991) *Eur. J. Biochem. 200*, 423−429.
60. Melander, L., and Saunders, W. H., Jr. (1987) *Reaction Rates of Isotopic Molecules*, 2nd ed., Robert E. Krieger Publishing Co., Malabar, FL.
61. Alston, W. C., Kanska, M., and Murray, C. J. (1996) *Biochemistry 35*, 12873−12881.
62. Bahnson, B. J., Park, D.-H., Kim, K., Plapp, B. V., and Klinman, J. P. (1993) *Biochemistry 32*, 5503−5507.
63. Basran, J., Sutcliffe, M. J., and Scrutton, N. S. (1999) *Biochemistry 38*, 3218−3222.
64. Kwart, H. (1982) *Acc. Chem. Res. 15*, 401−408.
65. Schneider, M. E., and Stern, M. J. (1971) *J. Am. Chem. Soc. 93*, 1517−1522.
66. Bell, R. P. (1980) *The Tunnel Effect in Chemistry*, Chapman & Hall, New York.
67. Kohen, A., and Klinman, J. P. (1999) *Chem. Biol. 6*, R191−R198.
68. Marcus, R. A., and Sutin, N. (1985) *Biochim. Biophys. Acta 265*, 265−322.
69. Dogonadze, R. R., Kuznetsov, A. M., and Levich, V. G. (1967) *Electrokhimiya 3*, 739−742.
70. Johnson, H. S., and Rapp, D. (1961) *J. Am. Chem. Soc. 83*, 1−9.
71. Alhambra, C., Corchado, J. C., Sanchez, M. L., Gao, J. L., and Truhlar, D. G. (2000) *J. Am. Chem. Soc. 122*, 8197−8203.
72. Cleveland, W. S. (1979) *J. Am. Stat. Assoc. 74*, 829−836.

BI020054G